Available online at www.sciencedirect.com
SCIENCE DIRECT
Polymer 46 (2005) 11798–11805
polymer
www.elsevier.com/locate/polymer

Rate mechanisms of plasticity in semi-crystalline polyethylene

A.S. Argon [a,*], A. Galeski [b], T. Kazmierczak [b]

[a] Massachusetts Institute of Technology, Cambridge, MA 02139, USA
[b] Centre of Molecular and Macromolecular Studies, Polish Academy of Sciences, Sienkiewicza 112, 90-363 Lodz, Poland

Received 31 January 2005; received in revised form 24 June 2005; accepted 27 June 2005
Available online 21 October 2005

Abstract

Based on our experiments on polyethylene where we have observed a constant level of plastic resistance, independent of lamella thickness exceeding 40 nm, we have fundamentally re-considered the rate controlling mechanisms of crystal plasticity in semi-crystalline polymers. In this we have not only re-examined and made modifications to the widely accepted mechanism of Young (Young RJ. Mater Forum 1988;11:210.) of monolithic nucleation of screw dislocations from edges of crystalline lamellae predicting an increase in plastic resistance with increasing lamella thickness, but we are proposing here two new modes of nucleation of both edge and screw dislocation half loops from lamella faces that are independent of lamella thickness. These two new modes of dislocation nucleation explain well the observed transition from a plastic resistance increasing with lamella thickness to one of constant resistance above a lamella thickness of ca. 35 nm in polyethylene. They also provide a more satisfactory framework to explain the temperature and strain rate dependence of the plastic resistance of polyethylene and predict the observed levels of activation volumes determined by us.

Keywords: Dislocation nucleation modes; Rate dependent plasticity; Polyethylene

1. Introduction

Plastic flow of semi-crystalline polymers and its rate mechanism, particularly in polyethylene has attracted much interest for decades. The large number of experimental studies probing the kinematics and kinetics of plastic deformation in polyethylene (PE) and some other semi-crystalline polymers of high levels of crystallinity has been reviewed thoroughly by Oleinik [1] and Galeski [2]. The overwhelming evidence, particularly in relation to formation of deformation-induced textures in compression flow where spurious cavitation processes are avoided is that this texture evolves by a series of crystallographic shears in the crystalline lamellae. The associated amorphous component separating lamellae is merely 'carried along' (Bartczak, et al. [3]) beyond the earliest forms of deformation where this component is merely stretched out and 'locked'. While the overall deformation of the assembly of crystalline lamellae and associated amorphous components has been successfully modeled by Lee, et al. [4] and more recently by van Dommelen et al. [5,6] using separately measured crystallographic glide resistances (Bartczak, et al. [7]) and deformation resistance of the amorphous component (Arruda and Boyce [8]), there is far less understanding of the rate processes of the crystallographic shears.

The overwhelming evidence accumulated over several decades is that the crystalline lamellae of PE, much like all crystalline ductile metals, deform plastically by the generation and motion of crystal dislocations and that while twinning and martensitic shears have also been suspected these do not make a substantial contribution. In coarse grained polycrystalline metals the rate mechanism of deformation is governed almost exclusively by either the intrinsic lattice resistance or the resistance of localized obstacles to dislocation motion. Dislocation nucleation in crystal plasticity as a rate controlling process is found only in nearly perfect crystals or in polycrystals in the nanoscale range.

In PE and similar semi-crystalline polymers with chain molecules aligned nearly normal to the wide surfaces of the crystalline lamellae the preferred systems are those of chain slip on planes with the largest interplane separation: (100) in PE; (001) in nylon-6. In such systems because of the very high stiffness of the chain molecules it can be expected that the width of the core of the edge dislocations would be very large, resulting in only a negligible lattice resistance, making

* Corresponding author.
E-mail addresses: argon@mit.edu (A.S. Argon), andgal@bilbo.cbmm.lodz.pl (A. Galeski).

0032-3861/$ - see front matter © 2005 Elsevier Ltd. All rights reserved.
doi:10.1016/j.polymer.2005.06.126

the screw dislocations with much narrower cores to be the most likely carriers of plasticity associated with the rate mechanism. That this had been so was confirmed indirectly by Peterman and Gleiter [9] who made the first TEM observations of screw dislocations in PE lamellae.

The possibility that glide mobility of screw dislocations might be rate controlling was studied by Lin and Argon [10] in highly textured nylon-6 quasi-single crystals where a generally convincing association was made to chain 'cross-overs' in the (001) planes as being the thermally penetrable obstacles to screw dislocation motion. Such chain 'cross overs' that are a topologically unavoidable product of large strain compression flow that was used to produce the quasi-single crystalline samples should, however, be largely absent in melt crystallized lamellae. For this and other reasons that the lamellae thicknesses are only in the nanoscale range (10–15 nm) it has been suspected for a long time that the rate controlling process must be repeated dislocation emission from lamellar edges under stress with the nucleated dislocations rapidly exiting the lamellae on the other side, requiring the process to repeat continuously. This process of emission of dislocations from the edges of the lamellae across the narrow faces that was initially proposed by Peterson [11] explored further by Shadrake and Guiu [12] and more rigorously by Young [13] has now been widely accepted. It was most recently re-examined by Brooks and Mukhtar [14]. In our experiments (Kazmierczak, et al. [15]) where PE with lamella thicknesses far exceeding the usual 10–15 nm (up to 170 nm) were studied, it became clear that when lamella thicknesses exceed 40 nm the mechanism of emission of screw dislocation lines from lamella edges must be superseded by another, more ubiquitous one that is no longer sensitive to lamella thickness.

It is this subject of the rate controlling process of dislocation emission from lamellar surfaces that is the subject of this communication. In examining new possibilities for which the fundamental considerations have been developed by Xu (Xu, et al. [16,17]; Xu and Zhang [18]; and Xu [19]), we also have re-visited the previous developments of screw dislocation emission monolithically from edges of thin lamellae and eliminated various questionable assumptions. We show that when this is done the previously proposed model of screw dislocation emission from lamella edges can provide results as accurate as the more rigorous developments of Xu, based on a variational boundary integral approach.

2. The rate controlling processes of plastic shear of lamellae

2.1. Overview

In PE, solidified from the melt the crystalline lamellae, separated by a thin amorphous component are arranged in spherulites (Lin and Argon [20]). The glide resistances in PE lamellae on slip systems of chain slip have been experimentally measured in highly textured PE of close to quasi single crystalline perfection by a number of researchers (Bartczak [7] and other references therein). At room temperature the system with the lowest shear resistance at a level of 7.5 MPa is the (100) [001] chain slip system. The resistances on other systems with slip directions parallel and perpendicular to the chain direction have also been measured and are known (Bartczak, et al. [7]). When spherulitic PE is plastically deformed, compatibility requires that systems other than the principal (100) [001] system also deform as required. Nevertheless, large strain texturing deformation experiments and computer simulation of the entire process of texture-producing flow (Lee et al. [4], van Dommelen, et al. [5,6]) show that the contribution of the (100) [001] system to the total plastic deformation is dominant and that its rate mechanism also dominates over all others. These simulation experiments demonstrate that the effective so-called Taylor factor (Taylor [21]) relating the uniaxial tensile or compressive plastic resistance to the slip resistance of the (100) [001] system is close to $m_T = 3.00$. Thus, in our consideration of the rate mechanism of plastic flow in individual lamellae we limit our attention to deformations resulting from shear on the (100) [001] system as depicted in Fig. 1(b), where for simplicity for stress considerations a lamellar crystal is depicted with its [100] direction pointing radially outward. While, this is counter to the usual known orientation of lamellae with their [010] direction parallel to the radial direction, this is unimportant for our consideration of the plastic deformation of individual lamellae. Thus, the principal local plastic deformation process is $d\gamma_{13}$ shear, promoted by the resolved τ_{13} shear stresses, referred to the PE orthorhombic crystal structure. We will consider plastic flow only in this limited context in a representative lamella, based on the well established preponderance of slip on the (100)[001] crystallographic system [4–6].

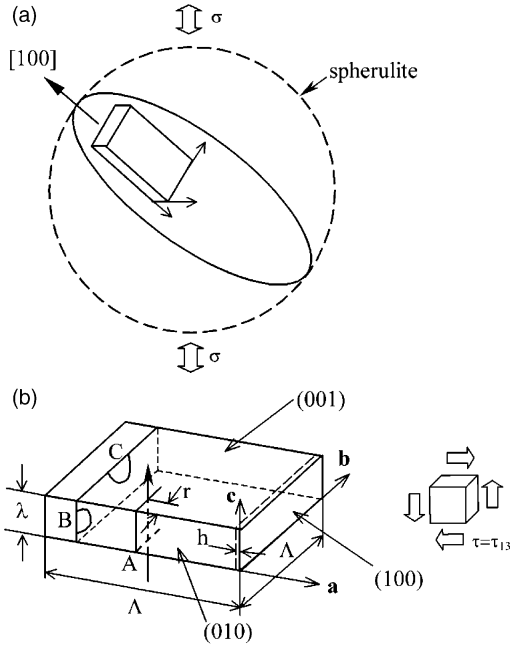

Fig. 1. Sketches depicting: (a) a typical lamella in a great circle in a spherulite; (b) geometry of a typical lamella showing the principal chain slip system (100) [001] and the three separate modes of dislocation nucleation: A monolithic screw, B screw half loop, and C edge half loop.

The principal mode of deformation in tension or compression is the thinning of the lamellae accomplished by increments of $d\gamma_{13}$ shear which we refer to from here on simply as $d\gamma$ and its rate as $\dot{\gamma}$, promoted by the τ_{13} shear stress to which we will refer to simply as τ. We will, by necessity, also consider well established secondary effects of how the shear resistance on the (100) [001] system is affected by a normal stress σ_{11} acting across it.

Fig. 1(b) depicts the representative lamella which we consider to be of lateral dimensions Λ in the range of 2.5 μm and thickness λ in the nm range. For simplicity we consider the molecular stems to be normal to the wide faces and equal in length to λ. While it has often been reported that the molecules are initially inclined with the lamella surfaces by angles around 30°, this will change up or down in the course of shearing of lamellae. Therefore, this initial form will be of no major concern in the analysis of activation configurations to be discussed below. Fig. 1(b) depicts three modes of dislocation nucleation-controlled processes of chain slip on the (100) [001] system. The process identified as A is the previously considered one of nucleation of a fully formed screw dislocation monolithically from the narrow face. Clearly, as the lamella thickness λ increases the ever increasing activation energy of this mode will no longer be kinetically feasible. Thus, we consider two other modes: a screw dislocation half loop nucleation, still from the narrow face, and an alternative process of edge dislocation half loop nucleation from the wide face, depicted as processes B and C, respectively, in Fig. 1(b). The energetics of all three processes has been considered rigorously by Xu (Xu and Zhang [18] and Xu [19]). We will make use of these developments but start by considering first the previously discussed mode A in a more rigorous way without any unnecessary approximations and will demonstrate that when so done the result will be exactly the same as the exact analysis of Xu and Zhang [18].

2.2. Nucleation of a screw dislocation in mode A

Since the mode of nucleation is a monolithic one along the entire edge, we consider the process first per unit length.

Thus, the Gibbs free energy change, ΔG, due to insertion of a fully formed screw dislocation from the edge by a critical distance r form the edge is

$$\Delta G = \Delta F - \Delta W = \frac{\mu b^2}{4\pi}\ln\left(\frac{\alpha r}{b}\right) - \tau b r \tag{1}$$

where we have introduced the core cut-off parameter α in the well-known way (Hirth and Lothe [22]) that accounts for the core energy in units of line energy outside the core. We determine the magnitude of α below. In Eq. (1) r is the single activation parameter which is determined by seeking the saddle point condition that maximizes ΔG, i.e.

$$\left(\frac{\partial \Delta G}{\partial r}\right)_{\tau} = 0 \tag{2}$$

which gives

$$r_c = \frac{\mu b}{4\pi\tau} \tag{3}$$

Thus, upon substitution into Eq. (1), this gives

$$\Delta G^* = \frac{\mu b^2}{4\pi}\ln\left(\frac{\alpha}{4\pi e}\frac{\mu}{\tau}\right) \tag{4}$$

where $e = 2.72$ is the Neperian number.

We consider

$$\tau_c = \frac{\mu}{(4\pi e/\alpha)} \tag{5}$$

as the ideal shear strength of the (100) [001] chain slip system which fixes the final form of ΔG^* (per unit length) to be

$$\Delta G^* = \frac{\mu b^2}{4\pi} g_A(\beta) \tag{6a}$$

where

$$g_A(\beta) = \ln\left(\frac{1}{\beta}\right) \tag{6b}$$

and

$$\beta = \frac{\tau}{\tau_c} \tag{7}$$

We note that if the ideal shear resistance of the (100) [001] slip system were given by a Frenkel sinusoid (Frenkel [23]) then the ideal shear strength of this system would be

$$\tau_c = \frac{\mu b}{2\pi h} \tag{8}$$

where h is the interplanar spacing of the (100) planes. Thus, equating Eqs. (5) and (8) establishes that

$$\alpha = 3.74 \tag{9}$$

which is in keeping with expectations for a basically covalent crystal. The stress dependent form of ΔG^* (per unit length) is

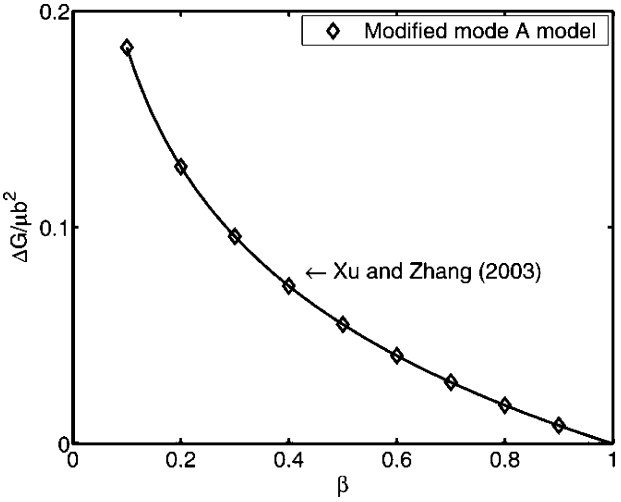

Fig. 2. Stress dependence of activation free energy of the mode of nucleation of a monolithic screw dislocation from a lamella edge, per unit length, Eqs. (6a) and (6b) represented by (◇), compared with the solution of Xu and Zhang [18].

plotted as the series of individual points in Fig. 2. The curve in the figure represents the finding of Xu and Zhang [18] obtained rigorously by a variational boundary integral method. The agreement is perfect.

If instead of considering the process on a per unit length basis, we apply it to a specific lamella of thickness λ the total activation free energy would be

$$\Delta G_{\mathrm{A}}^{*} = \frac{\mu b^3}{4\pi}\left(\frac{\lambda}{b}\right)\ln\left(\frac{1}{\beta}\right) \tag{10}$$

this will be the activation energy that we will consider in the kinetics of plastic flow as one of the alternatives. We consider next the two other alternatives B and C where the lamella thickness plays no role.

2.3. Nucleation of screw dislocation half loop in mode B

Plastic shear on the (100) [001] system in a lamella can also be initiated by the nucleation of a screw dislocation half loop from the narrow $\lambda x \Lambda$ face of the lamella. This process has been considered rigorously by the variational boundary integral method developed by Xu and Ortiz [24] earlier and applied to many problems such as emission of dislocations from crack tips, and the like, summarized recently by Xu [25]. The problem of interest here has been solved by Xu and Zhang [18] giving a stress dependence of the activation free energy of this mode that is shown in Fig. 3, as the upper curve. It is of the form

$$\Delta G_{\mathrm{B}}^{*} = \mu b^3 g_{\mathrm{B}}(\beta) \tag{11}$$

where β has the same meaning as in Eqs. (6b) and (7). A useful empirical representation of the function $g_{\mathrm{B}}(\beta)$ is

$$g_{\mathrm{B}}(\beta) = \frac{(1-\beta^{2/3})}{\beta^{1.25}} \tag{12}$$

We will use it comparing with experimental results. We note that $g_{\mathrm{B}}(\beta)\to 0$ when $\beta\to 1$ as it should.

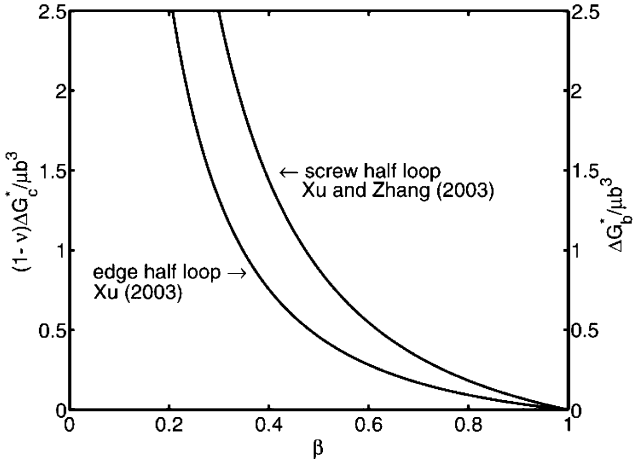

Fig. 3. Stress dependences of activation free energy of models of nucleation of screw dislocation half loops (from Xu and Zhang [18]) and edge half–half loops (from Xu [19]).

2.4. Nucleation of an edge dislocation half loop in mode C

This mode of dislocation half loop nucleation has also been considered by Xu [19]. For this the resulting dependence of the activation free energy $\Delta G_{\mathrm{C}}^{*}$ on the normalized shear stress β is shown in Fig. 3 as the lower curve. It is of the form

$$\Delta G_{\mathrm{C}}^{*} = \left(\frac{\mu b^3}{(1-\nu)}\right) g_{\mathrm{C}}(\beta) \tag{13}$$

where a useful empirical form for $g_{\mathrm{C}}(\beta)$ is

$$g_{\mathrm{C}}(\beta) = \frac{(1-\beta^{1/3})}{\beta^{1.15}} \tag{14}$$

which we will use also in comparing with experimental results.

3. The strain rate expression

The kinetic crystallographic shear strain rate expression encountered in crystal plasticity is (Kocks, et al. [26]).

$$\dot{\gamma} = \dot{\gamma}_0 \exp\left(-\frac{\Delta G^{*}(\beta)}{kT}\right) \tag{15}$$

in the range of β sufficiently far from zero where back fluxes of flow units can be neglected. The pre-exponential factor is

$$\dot{\gamma}_0 = b\rho_{\mathrm{m}} L \nu_{\mathrm{G}} \tag{16}$$

where b is the magnitude of the Burgers vector, ρ_{m} the mobile dislocation density, L the mean free path of the mobile dislocation between inception and demobilization at sinks and ν_{G} the frequency factor associated with the stress fluctuation attempting the nucleation process. Of these terms the one requiring amplification is the mobile dislocation density. It is made up of several terms. The number N of possible nucleation sites on the faces of the lamellae, the probability, p of a successful nucleation event at a site, the length l of the dislocation following the nucleation event, the level of crystallinity X in the representative volume of $\lambda\Lambda^2$, allocated to a lamellae. Then $N=(2\Lambda/h)$ where h is the interplanar spacing of the (100) planes, l is λ, giving

$$\rho_{\mathrm{m}} = \left(\frac{2\Lambda}{h}\right)\frac{pX\lambda}{(\lambda\Lambda^2)} \tag{17}$$

In all three cases the mean free path length is close to Λ, and the attempt frequency $\nu_{\mathrm{G}} \cong \nu_{\mathrm{D}}/20$, where ν_{D}, the lattice shear vibration frequency on the (100) plane in the [001] direction is estimated to be close to $6.12\times 10^{11}\ \mathrm{s}^{-1}$ and the factor 1/20 comes from the characteristic saddle point half loop diameter of $\sim 20b$. Thus, with these

$$\dot{\gamma}_0 = 2\left(\frac{b}{h}\right)pX\nu_{\mathrm{G}} \tag{18}$$

independent of lamella dimensions as it should. It is reasonable to choose $p\approx 0.1$ and evaluate $X\approx 0.9$ as it is in our experiments (Kazmierczak, et al. [15]).

Thus, the kinetic expression of Eq. (15) gives

$$\frac{mkT}{\Delta G_{0i}^{*}} = g_i[\beta] \tag{19}$$

where $m \equiv \ln(\dot{\gamma}_0/\dot{\gamma})$ with $\dot{\gamma}$ being the applied shear strain rate. The quantity m is quite close to 30 in all cases and the various ΔG_{0i}^{*} expressions are for the three cases given as:

$$\Delta G_{0A}^{*} = \frac{\mu b^3}{4\pi}\left(\frac{\lambda}{b}\right) \tag{20a}$$

$$\Delta G_{0B}^{*} = \mu b^3 \tag{20b}$$

$$\Delta G_{0C}^{*} = \frac{\mu b^3}{(1-\nu)} \tag{20c}$$

In determining the temperature dependence of the plastic resistances in uniaxial deformation the temperature dependence of the shear modulus $\mu = c_{55}$ is needed. Karasawa, et al. [27] provided such information based on theoretical force field methods. We show their calculated results for c_{55} as the upper curve in Fig. 4. Karasawa, et al. have compared their theoretical results for c_{55} at 4 K with calculated results of others using different approaches. These other results range down to as low as 1.27 GPa, from their result of 3.0 GPa for this elastic constant. Experimental results are generally limited to measurements of the Young's modulus at room temperature in highly oriented PE, stressed in the orientation direction. In such a set of in situ XRD experiments, measuring lattice elastic strains under applied stress in highly oriented (up to extension ratios of 400) PE, with initial crystallinity above 90%, Matsuo and Sawatari [28] measured Young's moduli no larger that 202 GPa at room temperature—compared with the calculated Young's modulus of 318 GPa of Karasawa, et al., i.e. only 63.5% of theoretical. The principal cause of this discrepancy is most likely attributable to lattice defects. This level of agreement between theoretical and experimental elastic properties appears to be wide-spread and is most likely reflected also in the specific crystal elastic constants. On this basis we have attenuated the temperature dependent theoretical elastic constant c_{55} of Karasawa, et al. by the same factor 0.635 for operational purposes in our comparisons of our predicted temperature dependent yield stresses with experiments. This attenuated result is also shown in Fig. 4 as the lower curve.

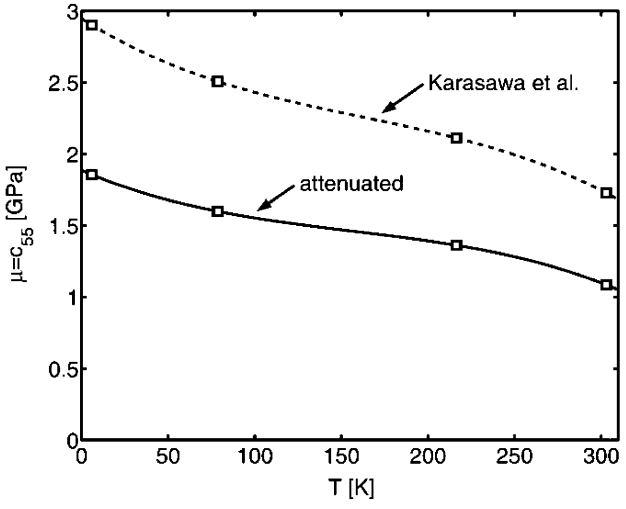

Fig. 4. Temperature dependence of the shear modulus $\mu = c_{55}$ of polyethylene from Karasawa, et al. [27], upper curve; lower curve shows above results, attenuated by a factor of 0.635, to reflect the best available experimental results (see text).

4. Activation volumes

The temperature dependence of the plastic resistance τ (or uniaxial resistance σ) and the activation volume are both very useful in probing the active mechanism.

The activation volume as determined from the models is given by

$$\frac{\Delta v^{*}}{b^3} = \frac{\Delta G_0^{*}}{b^3 \tau_c}\frac{\mathrm{d}}{\mathrm{d}\beta}(g(\beta)) \tag{21}$$

The specific forms for the three different modes A, B and C are

$$\left(\frac{\Delta v^{*}}{b^3}\right)_A = \frac{1}{4\pi}\left(\frac{\lambda}{b}\right)\left(\frac{\mu}{\tau_c}\right)\left(\frac{1}{\beta}\right) \tag{22a}$$

$$\left(\frac{\Delta v^{*}}{b^3}\right)_B = 1.25\left(\frac{\mu}{\tau_c}\right)\left(\frac{1-0.466\beta^{2/3}}{\beta^{2.25}}\right) \tag{22b}$$

$$\left(\frac{\Delta v^{*}}{b^3}\right)_C = \frac{1.15}{(1-\nu)}\left(\frac{\mu}{\tau_c}\right)\left(\frac{1-0.71\beta^{1/3}}{\beta^{2.15}}\right) \tag{22c}$$

For the sinusoidal interplanar ideal shear resistance, for all temperatures $(\mu/\tau_c) = 9.152$.

Experimentally the activation volume is determined operationally as:

$$\frac{\Delta v^{*}}{b^3} = \frac{kT}{b^3}\left(\frac{\mathrm{d}\ln\dot{\gamma}}{\mathrm{d}\tau}\right) = \frac{3kT}{b^3}\frac{\ln(\dot{\gamma}_2/\dot{\gamma}_1)}{\Delta\sigma} \tag{23}$$

where we have made use of the effective Taylor factor $\sigma/\tau_0 \cong 3.0$ (Lee, et al. [4]) relating the uniaxial resistance to the shear resistance τ_0 of the (100) [001] system.

5. Comparison with experiments

5.1. The dominant nucleation mode

In comparing the model results with experiments a number of factors need to be taken into account. These include the type of the PE, its molecular weight, branching content, crystallinity level and finally whether the experiments have been performed in tension or compression. Of these, our model accounts for lamella thickness, assumed to be the same as the molecule stem length, level of crystallinity and the tension and compression asymmetry. With regard to the latter we use the measurements of Bartczak, et al. [7] that demonstrated that lamella yielding on the (100) [001] system obeys a Coulomb law where the shear resistance τ is dependent on the normal stress σ_n acting

across the glide plane according to a relation

$$\tau = \tau_0 - K\sigma_n \tag{24}$$

where τ_0 is the resistance of the (100) [001] plane in simple shear and were $K=0.11$. While it is difficult to assess the collective normal stress effect on lamella of different angle of inclination in the spherulite, we make a correction based only on considering the effective slip planes at 45° with the uniaxial external stress state. On this basis to obtain the tensile flow stress we divide the calculated uniaxial flow stress with the factor $(1+K)$, and to obtain the compressive flow stress we divide the uniaxial flow stress by the factor $(1-K)$.

To identify the dominant rate controlling nucleation mode in the compressive yield experiments of Kazmierczak, et al. [15] on PE with different lamella thicknesses we determine the flow stresses of the three modes A, B and C by using Eqs. (7a), (12), (14), (19) and (20a)–(20c) to obtain

$$\sigma_i = \frac{m_T \tau_C}{(1-K)}\beta_i \tag{25}$$

where the specific β_i are obtained from

$$\beta_A = \exp\left(-\frac{4\pi mkT}{\mu b^3}\left(\frac{b}{\lambda}\right)\right) \tag{26}$$

and β_B and β_C from the solution of the non-linear equations

$$\beta_B^{2/3} + \left(\frac{mkT}{\mu b^3}\right)\beta_B^{1.25} - 1 = 0 \tag{27}$$

$$\beta_C^{1/3} + \left(\frac{(1-\nu)mkT}{\mu b^3}\right)\beta_C^{1.15} - 1 = 0 \tag{28}$$

We recall that $m_T=3$ is the effective Taylor factor relating the mechanism shear resistance to the uniaxial resistance as determined in the overall simulation of Lee, et al. [4], τ_C is the ideal shear strength given by Eq. (8), $m=\ln(\dot\gamma_0/\dot\gamma)$ which is close to 30 for all three cases as discussed in Section 3 above, and $K=0.11$ as also stated above. Of these results only σ_A depends on the lamella thickness while σ_B and σ_C do not. They are all plotted in Fig. 5. The data points are those of Kazmierczak, et al. [15] and show that they fall in between the models for nucleation of edge half loops and screw half loops. The model suggests a sharp departure from the mode of monolithic screw dislocation line nucleation to the half loop modes at roughly around 16 nm lamella thickness. The experiments show a more gradual transition at a lamella thickness of roughly 28 nm. Considering the quite mixed population of lamella thickness shown in the SEM micrographs of Fig. 4(a)–(c) in Kazmierczak, et al. [15] this more gradual transition is quite reasonable.

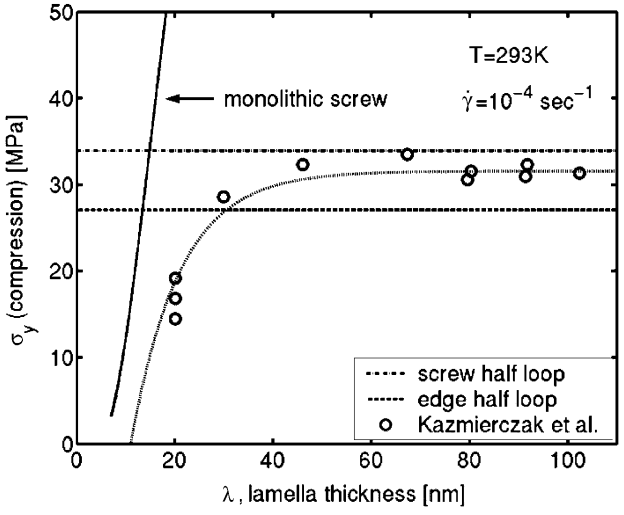

Fig. 5. Dependence of compressive flow stress of polyethylene at 293 K and $\dot\gamma=10^{-4}$ s^{-1} on lamella thickness: compared with theoretical models.

5.2. Temperature dependence of the plastic resistance

To probe the models further we compare the predicted temperature dependence of the tensile plastic resistance with the recent experimental results of Brooks and Mukhtar [14]. We choose for comparison their material PE2 of 206 k weight average molecular weight with a crystallinity of only 0.538 and molecular stem length of 13.2 nm, which we take as the lamella thickness as assumed in our model. For the predictions, using the same set of Eqs. (25)–(28) we use a factor of $(1+K)$ in the denominator in Eq. (25) since the experiments were performed in tension. The calculated temperature dependent tensile resistances are plotted in Fig. 6 for these modes of monolithic screw dislocation emission from lamella edges and those of edge and screw half loop emissions from the large and small faces of the lamellae, respectively. The data points of Brooks and Mukhtar lie along a band that parallels the half loop nucleation modes and not the model of the usually considered mode of nucleation of monolithic screw dislocations. However, they lie considerably below the models of the half loop nucleation. The discrepancy is partly due to the relatively low level of crystallinity of $X=0.538$

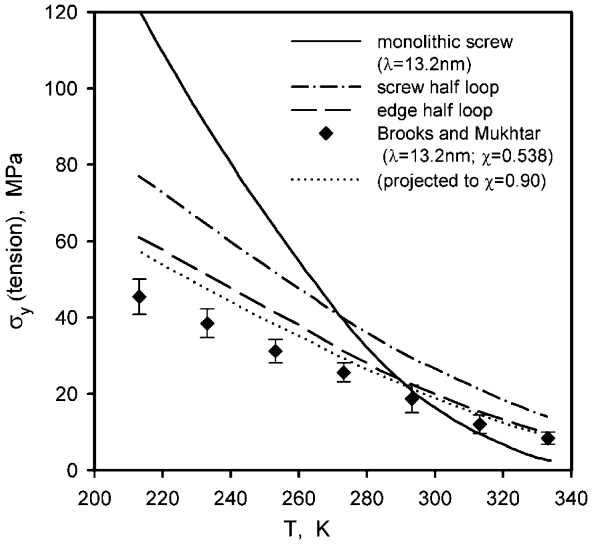

Fig. 6. Predictions of modes A, B, and C models of dislocation nucleation for the temperature dependence of the tensile yield stress of polyethylene compared with experimental results of Brooks and Mukhtar [14] for their PE2 material of moderate level of crystallinity at $X=0.538$. Dotted curve projects experimental results for $X=0.9$.

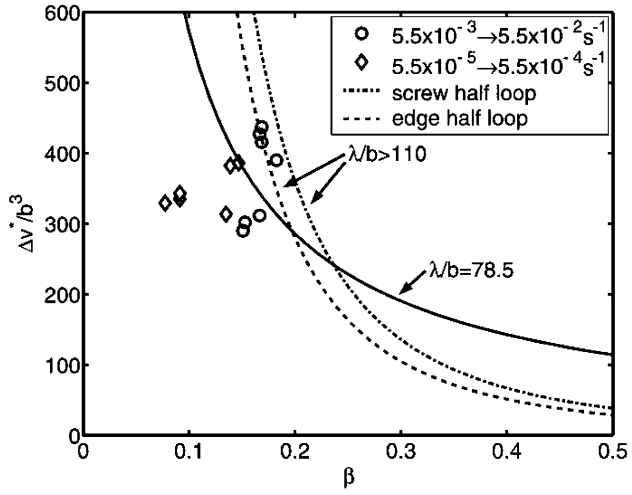

Fig. 7. Model predictions of stress dependence of normalized activation volumes compared with experimental results of Kazmierczak et al. [15] for up-jump experiments of strain rate change.

in PE2 while the models considered $X=0.90$. If the data were to be modified for a crystallinity of 0.9 the experimental band of points would move up to the dotted curve lying much closer to the model of nucleation of edge dislocation half loops. We note that from the predictions of Fig. 6, for thinner lamellae, while it may be possible to consider that at room temperature and above, the flow stress might be governed by the mechanism of monolithic emissions of screw dislocations, the mechanism can switch over to that of half loop nucleation at lower temperatures.

5.3. The activation volumes

Finally, we compare the activation volumes predicted by the models with some of those measured by Kazmierczak, et al. [15] in strain rate jump experiments. The activation volumes normalized by b^3, calculated from the model expressions of Eqs. (22a)–(22c) are shown in Fig. 7 where the model calculation for the nucleation of monolithic screw dislocation emissions was based on $\lambda=20$ nm. The data for 13 'up-jump' strain rate change experiments are also plotted on Fig. 7. The details of these experiments are given elsewhere (Kaxmierczak, et al. [15]). The measured $\Delta\nu^*/b^3$ for the jump experiments from $\dot{\gamma}=5.5\times10^{-3}$ to 5.5×10^{-2} fall quite close to the models for nucleation of dislocation half loops. The data for jumps at considerably lower strain rates and smaller flow stresses fall a bit closer to the model of nucleation of monolithic screw dislocations but are in much less satisfactory agreement. In all cases it was assumed that the externally applied stresses directly apply locally, which considering the generally confused morphology of packing of lamellae in a sphereulite is probably not the case and some level of local stress concentration among lamellae is very likely present. This would shift the measured data toward the right. However, the measured activation volumes are generally in the correct range.

6. Discussion

While the rate controlling processes of plastic flow in glassy polymers has seen considerable attention in the past (for an overview see Argon [29]), those in semi-crystalline polymers have seen much less attention beyond the model of Young [13] based on nucleation of screw dislocations monolithically from edges of lamellae. Our experiments (Kazmierczak, et al. [15]) with PE containing lamellae of much larger thicknesses than those of 10–15 nm, that are encountered most commonly in melt crystallized PE, have forced a re-examination of not only the model of Young, most recently considered again by Brooks and Mukhtar [14] but also other alternatives that must take over for thicker lamellae. These new alternatives consisting of nucleation of either screw or edge half loops of dislocations from the narrow and wide faces, respectively, of lamellae have been developed in the present communication. In the re-examination of the model of monolithic nucleation of screw dislocations we have found that even this model had not been treated rigorously enough in the past. A more uncompromising treatment, of this model, making no unjustifiable assumptions or simplifications has given results that are precisely the same as the more recent and rigorous treatments of problems of dislocation nucleation from a flat surface developed by Xu and Zhang [18] using a variational boundary integral method, (for a summary of this technique used for such problems see Xu [25]).

Using the results of Xu [19] and Xu and Zhang [18] we have proposed in the present communication two alternative modes of nucleation of screw and edge dislocation half loops from the thin and wide surfaces of lamellae as rate controlling processes of plastic deformation in PE and, by extension, of other semi-crystalline polymers having spherulite morphology. These two alternatives that are no longer dependent on lamellae thickness have explained well the transition of the plastic resistance to constant levels for lamellae of thickness exceeding roughly 20 nm, from resistances increasing with increasing lamella thickness encountered when the latter are less than 20 nm. The new alternatives are in far better agreement with the published temperature dependences of the plastic resistance of PE than the previous model of Young and also predict well the measured levels on activation volume. Thus noting from Fig. 7 that the mean level of activation volumes were of the order of $350b^3$ we estimate the typical radius of the dislocation half loop to be $r^*=b(700/\pi)^{1/2}=3.8$ nm, and much smaller indeed than the critical lamella thickness of 20 nm (40 nm experimental) where the flow stress becomes independent of lamella thickness. These new developments have provided a much better level of understanding of the rate controlling process of plastic deformation in semi-crystalline polymers and go a long way in providing additional solid support for the dominance of crystal plasticity as the central deformation mechanism in semi-crystalline polymers of high levels of crystallinity.

It is also pleasing to note that the present findings on the dominance of a dislocation nucleation-controlled mechanism of crystal plasticity in the assemblies of lamellae in the nm range of thicknesses is in keeping with similar findings of the

plasticity in nano-structured polycrystalline metals. It is noted that in the latter, while substantial strain is produced by grain boundary shear the rate mechanism is governed by the emission of dislocations from stress concentrations at grain boundary junctions that make up the principal mechanism of accommodation required by compatibility. The present findings leave also in tact the previous observations that plasticity in highly textured semi-crystalline polymers of quasi-single crystalline perfection and long range coherence may still be controlled by dislocation mobility (Li and Argon [10]) where the rate controlling glide obstacles were found to be the chain cross-overs in the highly aligned morphology where little evidence was found for a remaining lamellae morphology (Schőnherr, et al. [30]).

Acknowledgements

A.S.A. acknowledges useful discussions with Prof D.M. Parks and support of the Mechanical Engineering Department at MIT while AG acknowledges the support of grant KBN-7-T08E-055-22 and a PhD grant KBN-7-T08E-017-21 for T.K., both from the State Committee for Scientific Research of Poland.

References

[1] Oleinik E. Polym Sci Ser C 2003;45:17.
[2] Galeski A. Prog Polym Sci 2003;28:1643.
[3] Bartczak Z, Galeski A, Argon AS, Cohen RE. Polymer 1996;37:2113.
[4] Lee BJ, Argon AS, Parks DM, Ahzi S, Bartczak Z. Polymer 1993;34:3555.
[5] van Dommelen JAW, Parks DM, Boyce MC, Brekelmans WAM, Baaijens FPT. Polymer 2003;44:6089.
[6] van Dommelen JAW, Parks DM, Boyce MC, Brekelmans WAM, Baaijens FPT. J Mech Phys Solids 2003;51:519.
[7] Bartczak Z, Argon AS, Cohen RE. Macromolecules 1992;25:5036.
[8] Arruda EM, Boyce MC. J Mech Phys Solids 1993;41:389.
[9] Petermann J, Gleiter H. Philos Mag 1972;25:813.
[10] Lin L, Argon AS. Macromolecules 1994;27:6903.
[11] Peterson JM. J Appl Phys 1966;37:4047.
[12] Shadrake LG, Guiu F. Philos Mag 1976;34:565.
[13] Young RJ. Mater Forum 1988;11:210.
[14] Brooks NWJ, Mukhtar M. Polymer 2000;41:1475.
[15] Kazmierczak T, Galeski A, Argon AS. Polymer 2005;46:8926.
[16] Xu G, Argon AS, Ortiz M. Philos Mag A 1995;72:415.
[17] Xu G, Argon AS, Ortiz M. Philos Mag A 1997;75:341.
[18] Xu G, Zhang C. J Mech Phys Solids 2003;51:1371.
[19] Xu G. Philos Mag A 2002;82:3177.
[20] Lin L, Argon AS. J Mater Sci 1994;29:294.
[21] Taylor GI. J Inst Met 1938;62:307.
[22] Hirth JP, Lothe L. Theory of dislocations. 2nd ed. New York: Wiley; 1982.
[23] Frenkel JZ. Physik 1926;37:572.
[24] Xu G, Ortiz M, Interm J. Num Meth Eng 1993;36:3675.
[25] Xu G. In: Nabarro FRN, editor. Dislocations in solids, vol. 12. Amsterdam: Elsevier; 2004. p. 81.
[26] Kocks UF, Argon AS, Ashby MF. In: Chalmers B, Christian JW, Massalski TB, editors. Progress in materials science, vol. 19. Oxford: Pergamon Press; 1975.
[27] Karasawa N, Dasgupta S, Goddard III WA. J Chem Phys 1991;95:2260.
[28] Matsuo M, Sawatari C. Macromolecules 1986;19:2260.
[29] Argon AS. In: Cahn RW, Haasen P, Kramer EJ, editors. Materials science and technology, vol. 6. Germany: WCH, Weinheim; 1993. p. 461.
[30] Schőnherr H, Vancso GJ, Argon AS. Polymer 1995;36:2115.